

## Field Test and Thermal Performance Comparison of a Novel Underground Thermal Battery with a Single U-tube Borehole Heat Exchanger for Geothermal Heat Pump Application \*

Sajjan Pokhrel<sup>1</sup>, Xiaobing Liu<sup>1</sup>, Yu-Feng Lin<sup>2,3</sup>, Andrew Stump<sup>2</sup>, Ming Qu<sup>4</sup>, and Tim Mies<sup>5</sup>

1: Oak Ridge National Laboratory, Oak Ridge, Tennessee

2: Illinois State Geological Survey, University of Illinois Urbana-Champaign

3: Illinois Water Resources Center, University of Illinois Urbana-Champaign

4: Lyles School of Civil and Construction Engineering, Purdue University

5: Energy Farm Operations, University of Illinois Urbana-Champaign

[pokhrels@ornl.gov](mailto:pokhrels@ornl.gov), [liux2@ornl.gov](mailto:liux2@ornl.gov)

**Keywords:** geothermal heat pump, underground thermal battery, borehole heat exchanger, renewable heating and cooling

### ABSTRACT

Geothermal Heat Pumps (GHP) are a proven technology to efficiently provide space heating and cooling by utilizing the thermally stable subsurface of the ground as a heat sink or heat source. However, the high drilling costs of conventional borehole heat exchangers (BHEs) associated with GHP systems and subsurface heterogeneity have been two barriers hindering widespread adoption of GHPs. In this paper, we present results from a field test of an Underground Thermal Battery (UTB) as a potential alternative to a conventional BHE. To benchmark the UTB performance, a side-by-side field test was conducted to compare the UTB with a conventional BHE installed at the same site. The UTB was installed in a 7.01-meter-deep borehole having a diameter of 0.9 meter, whereas the conventional BHE (with single U-tube loop) is in a borehole with 36.6-meter depth and 0.15-meter diameter. Both are integrated into a GHP system to meet the thermal demands of an office space at the Illinois Energy Farm on the University of Illinois Urbana-Champaign campus. The system's performance is compared in terms of heat transfer rate, outlet temperatures, and contributions to the overall thermal power of the ground heat exchanger under varying thermal demands and in different heat pump operation modes: heating only, cooling only, and hybrid (alternative, diurnal heating and cooling). Results to date indicate that the UTB delivers a more consistent outlet temperature during a period of varying thermal demands. Its performance is better than the conventional BHE during short-term with higher thermal demands, while the conventional BHE performs better under continuous, lower thermal demands.

### 1. INTRODUCTION

The adoption of geothermal heat pumps (GHPs) offers numerous advantages. Nationwide mass deployment of GHPs can save energy, reduce carbon emissions, defer the need for installing new electricity transmission lines, while creating jobs and improving public health [1]. However, the higher upfront cost of installing GHP systems remains a significant barrier to their widespread adoption [2]. The primary contributor to this cost is for drilling boreholes, which usually accounts for over 50% of the total system installation cost [3]. To make the technology more affordable, further research is needed to develop low-cost ground heat exchangers (GHEs).

Previous research in developing alternative GHEs beyond the conventional BHE, including using the coaxial or spiral heat exchangers and horizontal loop configurations [4] [5] [6] [7] [8]. One promising technological development that combines a helical heat exchanger with a thermal storage unit is the Underground Thermal Battery (UTB), a new GHE developed at the Oak Ridge National Laboratory (ORNL) over the past few years. The UTB can function both as a GHE and a thermal energy storage device. Earlier research on the UTB focused on various aspects, including lab-scale prototype development and thermal performance assessment [9], numerical model development and validation [10], development of a new g-function for the UTB [11], performance evaluation during charging and discharging cycles [12], and its effect on building electric demand [13].

The next step toward the commercialization of the UTB is the current field test at the Illinois Energy Farm on the University of Illinois Urbana-Champaign campus. The UTB is a component of a new GHP system, which includes a heat pump and three other conventional BHEs. The GHP system was commissioned in May 2024. The GHP system replaces an existing 3-ton conventional air conditioning unit and a furnace consuming propane, which provided cooling and heating to roughly half of a building. The other half of the building remains connected to the original heating and cooling system. A data acquisition system has been set up at the site with remote monitoring capabilities. The GHP system is implemented to provide a side-by-side comparison between the UTB with conventional BHEs under

---

\* This manuscript has been authored by UT-Battelle, LLC, under contract DE-AC05-00OR22725 with the US Department of Energy (DOE). The US government retains and the publisher, by accepting the article for publication, acknowledges that the US government retains a nonexclusive, paid-up, irrevocable, worldwide license to publish or reproduce the published form of this manuscript, or allow others to do so, for US government purposes. DOE will provide public access to these results of federally sponsored research in accordance with the DOE Public Access Plan (<http://energy.gov/downloads/doe-public-access-plan>).

identical geological and thermal conditions. For this study, performance is compared between the UTB and one of the three conventional BHEs (single U-tube in a 120 ft deep borehole). The other two conventional BHEs are not compared in this study.

## 2. SYSTEM SCHEMATICS AND WORKING PRINCIPLE

As shown in Figure 1 (d), the UTB and a conventional BHE, referred as W1 in this study, are installed adjacent to each other, with a 54.9 m (180 feet) distance between them. Both are connected to the GHP. The UTB was installed in a shallow borehole with 7.01 m (23 feet) in depth and 0.91 m (3 feet) in diameter, while the BHE was installed in a borehole with a depth of 36.6 m (120 feet) and a diameter of 0.15 m (0.5 feet) (Figure 1b).

W1 uses a single U-tube heat exchanger made with high-density polyethylene (HDPE). One leg of the U-tube serves as the inlet, while the other functions as the outlet. The UTB is comprised with a tank made with a corrugated HDPE pipe and a helical heat exchanger made with flexible cross-linked polyethylene (PEX) attached to the interior wall of the tank (Figure 1c). The helical heat exchanger spirals from the top to the bottom of the tank and back to the top through a straight pipe. For the current study, the tank is filled with water. A mixture of propylene glycol and water (in 70/30 ratio) circulates through the helical heat exchanger, exchanging heat with the water inside the tank, which in turn exchanges heat with the surrounding ground formation. To monitor temperature within the UTB, two thermocouple trees are installed. Each tree contains 10 thermocouples evenly spaced along the vertical axis, providing detailed measurements of temperature variation within the tank.

The heat transfer fluid in the UTB and W1 is individually controlled to maintain at a specified flow rate. The inlet and outlet temperatures, as well as the flow rate of the UTB and W1 are measured continuously in every minute, and the values are averaged over 15-minute intervals.

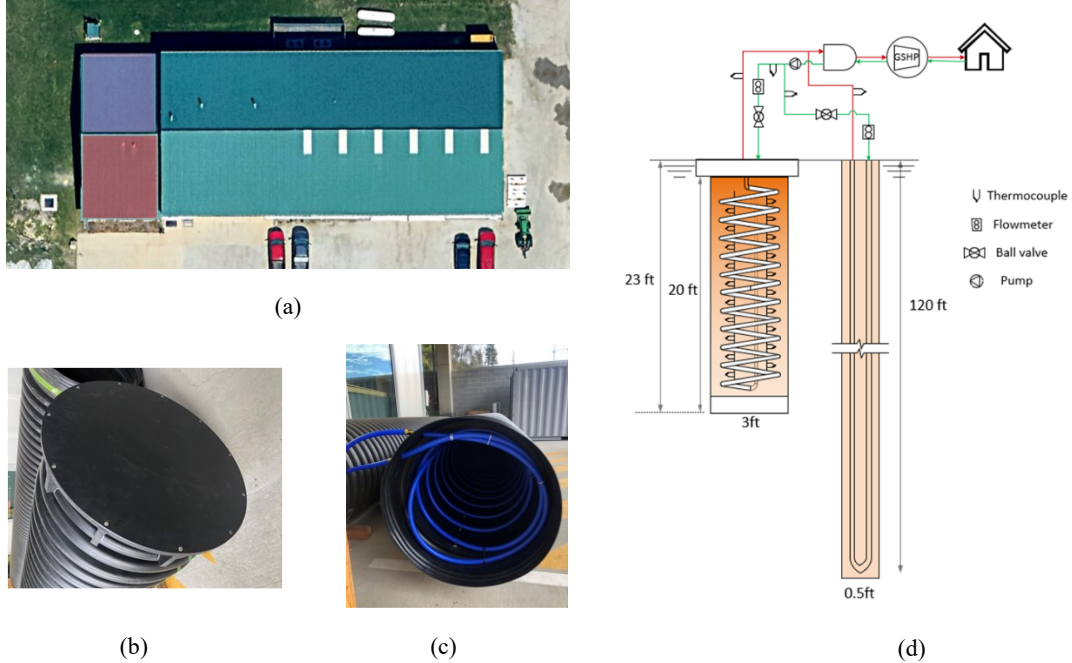


**Figure 1: (a) Satellite view of the field-test site (blue-shaded area is served by GHP and red-shaded area is served by conventional heating and cooling system); (b) UTB tank with bottom attached on a corrugated HDPE pipe; (c) PEX pipe attached on the interior wall of the UTB; and (d) a schematic of the field test set up.**

The W1 and UTB have an equal borehole surface areas of 20 square meters in contact with the surrounding ground to ensure an equal comparison between the two. The GHP system was commissioned in May 2024, and periodic testing was conducted for the first month. This study presents results from the first seven months of operation (June 2024 through December 2024). During this time, while the inlet temperature to W1 and UTB remained identical, the mass flow rate was intentionally varied to evaluate its impact on the performance.

## 3. GOVERNING EQUATIONS

The heat transfer rate of UTB and W1 is calculated using Equation (1), where  $T_{in}$  and  $T_{out}$  are the measured inlet and outlet temperatures ( $^{\circ}\text{C}$ ),  $\dot{m}$  is the measured mass flow rate ( $\text{kg/s}$ ), and  $C_p$  is the specific heat of the glycol, assumed an constant of 4186 J/Kg-K.

$$\dot{Q} = \dot{m}C_p(T_{in} - T_{out}) \quad (1)$$

The percentage to total heat transfer rate contributed from UTB and W1 is calculated using Equation (2). In Equation (2), the contribution is represented as  $\dot{Q}_{th}$  contribution (%). The heat transfer rate of UTB and W1 is represented by  $\dot{Q}_{delivered \ by \ W1 \ or \ UTB}$  (watts) and the total heat transfer rate is given by  $\dot{Q}_{delivered \ total}$  (watts).

$$\dot{Q}_{th} \text{ contribution (\%)} = \frac{\dot{Q}_{delivered \ by \ W1 \ or \ UTB}}{\dot{Q}_{delivered \ total}} \times 100 \quad (2)$$

The daily heating and cooling percentages are calculated as the ratio of time the GHP system operates in heating or cooling mode for a specific day as expressed in Equation (3).

$$\text{Daily heating or cooling (\%)} = \frac{\text{Total duration of heating or cooling}}{\text{Total duration of system operation}} \times 100 \quad (3)$$

## 4. RESULTS

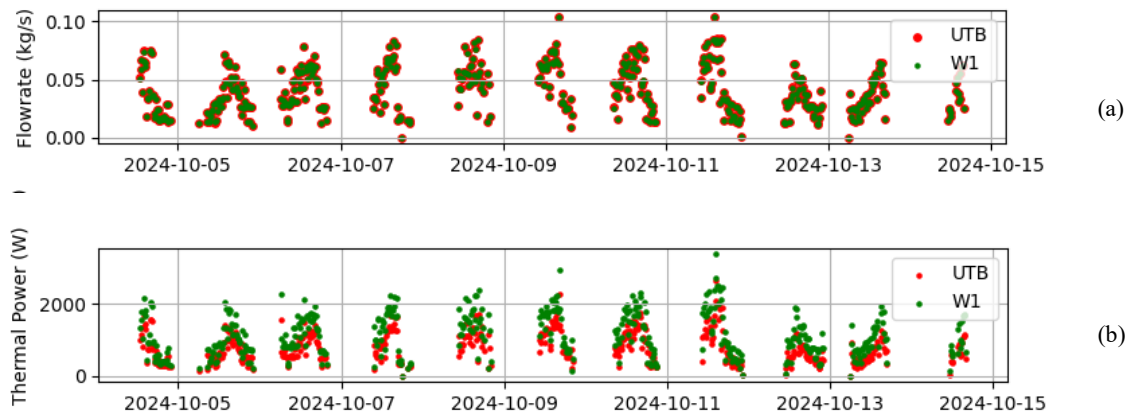
The field test results from June to December 2024 are presented this section. The GHP system was operated automatically during this period to maintain the room temperature at its setpoint. The GHP was switched into heating mode when the room temperature fell below 20.6°C (69°F) and into cooling mode when the room temperature rose above 23.3°C (74°F). To analyze the data according to the operation mode, the period was subdivided into cooling mode (from June 7 to October 25) when the GHP system was exclusively used for cooling, hybrid mode (from October 26 to November 14) when the system operated alternatively in heating and cooling modes, and heating mode (from November 15 to December 31) when space heating was the primary use.

### 4.1 Cooling mode

Two scenarios are analyzed for cooling mode operation: identical and different flow rates at the UTB and W1. The first scenario (identical flow rate) is to compare UTB and W1 under same operating conditions, and the second scenario (different flow rates) is to investigate the impact of flow rate on the heat transfer performance.

#### 4.1.1 Performance comparison under identical flow rate

Identical flow rates were maintained at UTB and W1 between October 4 and 15, 2024. The measured performance data, including flow rates, outlet temperatures, heat transfer rate, and instantaneous contribution percentages of UTB and W1 are shown in Figure 2. The instantaneous contribution,  $\dot{Q}_{th}$  contribution (%), indicates the percentage of the total heat transferred into the ground that is contributed by W1 and the UTB. The summation of the contribution percentages is 100%. As shown in Figure 2, the outlet temperature from W1 is lower than that from the UTB, which is also reflected by larger heat transfer rate and contribution of W1 over UTB. Figure 2(c) shows that UTB has relatively better performance (higher contribution) during and after increasing the thermal loads. This is due to the thermal buffer of the UTB that slows the change in outlet temperature of UTB. The average contribution during this period was 58.8% for W1 and 41.2% for the UTB.



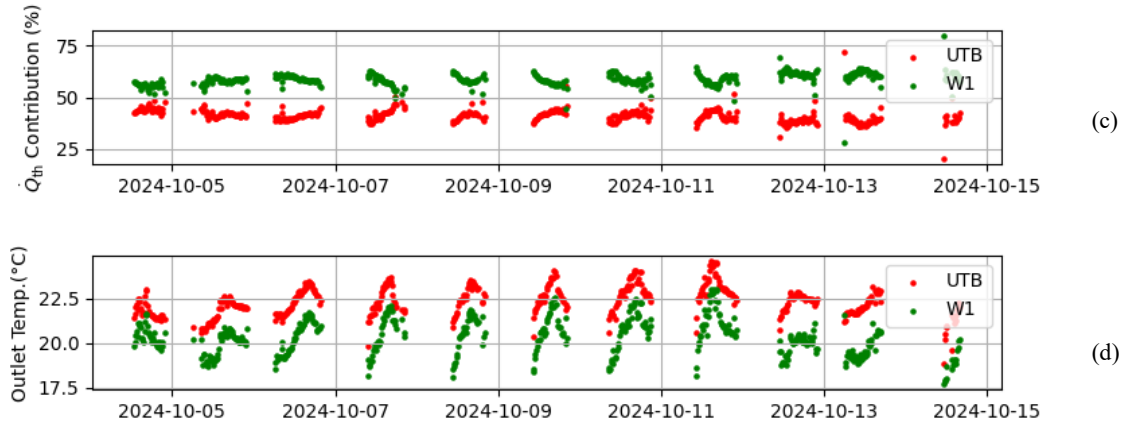


**Figure 2: Comparison between UTB and W1 when both ran at identical flow rate: (a) flow rate, (b) heat transfer rate, (c) contribution, and (d) outlet temperature.**

#### 4.1.2 Impact of flow rate on heat transfer rate

Field test results indicate that the heat transfer rate of the UTB and W1 is strongly affected by both the flow rate and the inlet temperature. Because these two inputs are not mutually exclusive, the results are normalized in terms of heat transfer rate per unit flow rate. Figure 3 shows this comparison, along with the trendlines between the inlet temperature and the normalized heat transfer rate for UTB and W1, respectively. Seven cases with different mass flow rates and inlet temperatures were plotted in Figure 3. Figure 4 presents the ratio of the mass flow rates between W1 and UTB in these cases.

On average, W1 has a higher normalized heat transfer rate than UTB. However, the ratio of heat transfer rate between W1 and UTB decreases as the inlet temperature increases. For instance, cases 3 and 7 have similar flow rate ratios, but the inlet temperature at case 7 was 26.8°C compared to 20.7°C at case 3. The ratio of heat transfer rate between W1 and UTB was 4.4 at case 3, while it was only 1.4 at case 7. In case 6, the normalized heat transfer rate of the UTB and W1 was the same, due to a higher flow rate in W1 than that in UTB (flow rate ratio is 2.12).

The results shown in figures 3 and 4 indicate that although W1 generally outperforms UTB, higher inlet temperatures, which reflect higher thermal loads, favor the performance of the UTB. It is thought to be due to the large thermal buffer of the UTB, which slows the change of outlet temperature of UTB.

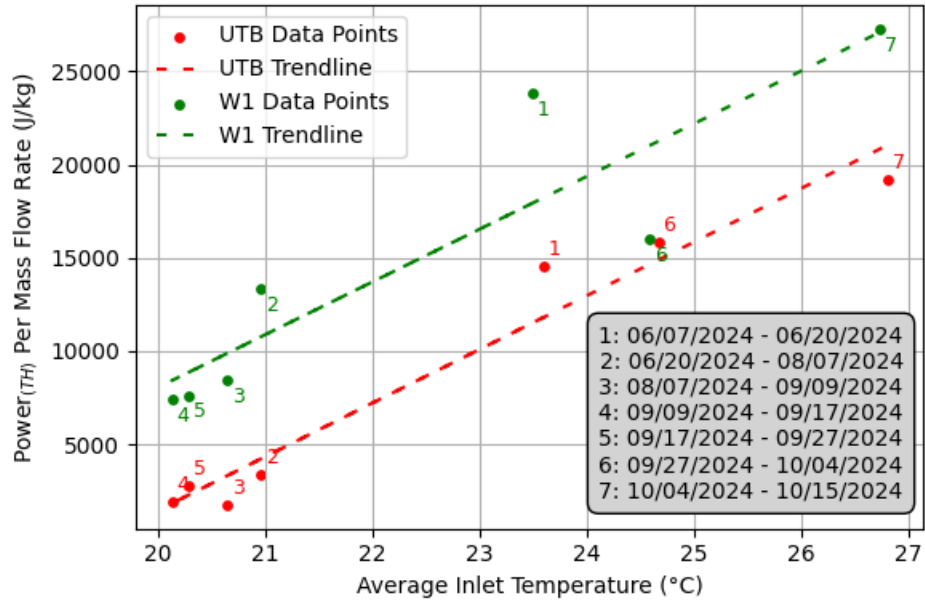


**Figure 3: Thermal power per unit flow rate vs. inlet temperature. The trendlines show correlation.**

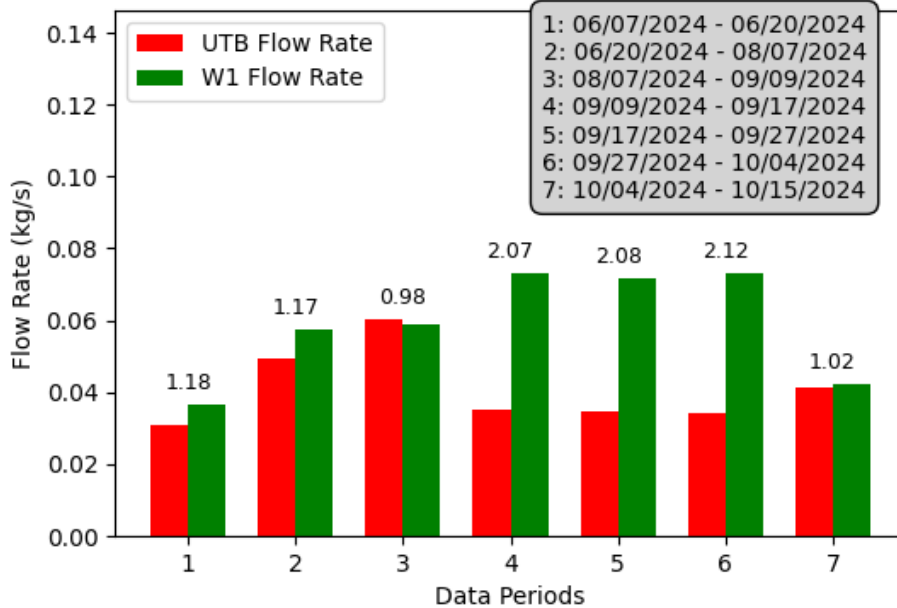
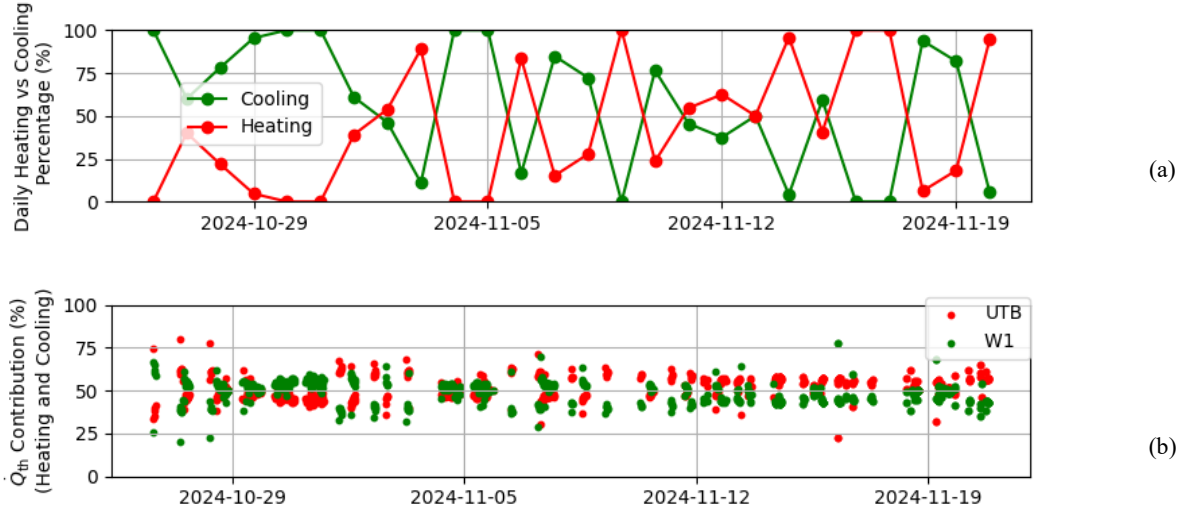


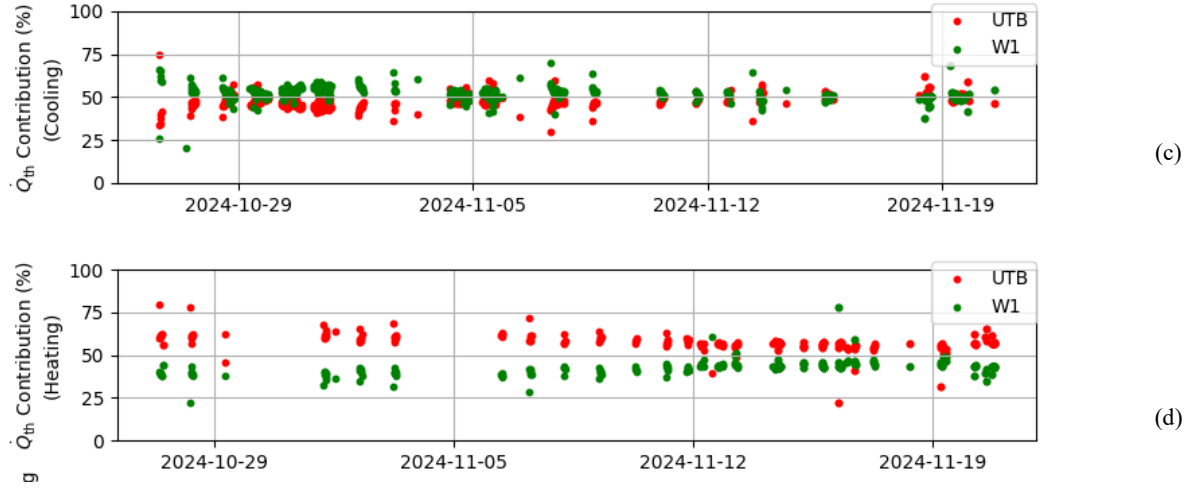
Figure 4: Flow rate comparison between UTB and W1 for all scenarios.

#### 4.2 Hybrid mode

From October 26 to November 21 in 2024, alternating heating and cooling operations were observed each day. During this period, the GHP provided heating in the early mornings and late evenings, while cooling was provided during the daytime when the ambient temperature rose. Furthermore, in few other days, either heating or cooling occurred for more than 90% of day. Data for these days were not included under hybrid operational mode. In Figure 5(a), the proportions of the days when heating or cooling occurred are shown. In Figures 5(b), 5(c) and 5(d), the contributions of heat transfer by UTB and W1 are shown. As shown in the Figure 5(a), the cooling demand was dominant during the first several days, while proportion of heating gradually increased in other days of this period.

Both UTB and W1 contributed significantly during this period, although UTB performed marginally better than W1. In the early several days, when the cooling demand was dominant, W1 outperformed UTB. However, as the time progressed and heating became more prevalent, the UTB started to outperform W1. Overall, UTB contributed 51% of the total heat transfer during this period and the rest was from W1. To better understand the heating and cooling performance between UTB and W1, further insights are presented in Figure 5(c) and Figure 5(d). In Figure 5(c), the heat transfer contributions during the cooling mode are shown, whereas in Figure 5(d) the contributions during heating are shown. For cooling operation, W1 initially performed better, but the benefits gradually diminished over time, with the UTB eventually outperforming W1 by the end of this period. For the heating operation, UTB outperformed W1 consistently, although the difference in performance diminished over time.

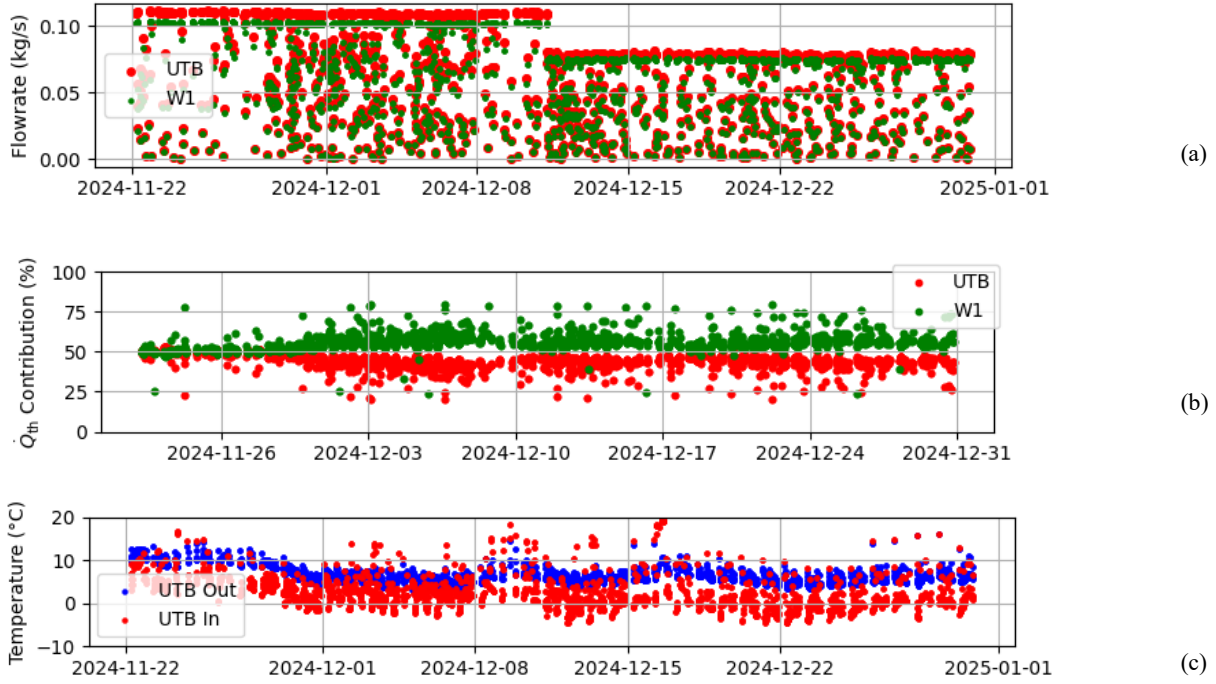




**Figure 5. Daily distribution of heating and cooling load (a), and performance comparison between UTB and W1 during the hybrid mode (b), (c), (d).**

#### 4.3 Heating mode

After November 22, 2024, the ambient air temperature dropped and the heating demand in the office space increased. The results of heating operation are shown in Figure 6. During this period, the flow rate was nearly identical in both W1 and UTB, as shown in Figure 6(a), with only a slightly higher flow rate in the UTB. This discrepancy is due to the limitation of the flow controller at the W1. The heat transfer contributions from UTB and W1 are presented in Figure 6(b), and the inlet and outlet temperatures at the two heat exchangers are shown in Figures 6(c) and 6(d). During the first several days of the heating operation, the heat transfer rate of W1 and the UTB was similar. However, as heating became dominant and thermal energy was continuously drawn from the ground, W1 demonstrated better performance than the UTB. We also determined that the UTB performance recovered after a short break or less frequent operation on December 10 and December 17. On average, 55.5% of the heat extraction was contributed by W1, while the rest was from the UTB.



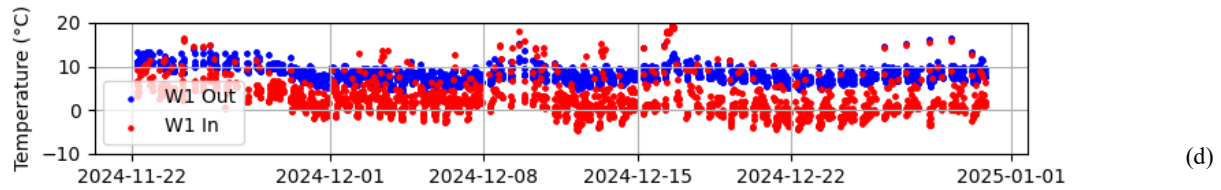


**Figure 6: Performance comparison during heating operation: (a) flow rates, (b) heat transfer contributions, (c) UTB inlet and outlet temperatures, and (d) W1 inlet and outlet temperatures.**

## 6. CONCLUSIONS

This study presents a field test of two GHEs: a conventional BHE (W1) and a UTB. Heat transfer performance of the two GHEs was compared during three modes: cooling, hybrid (alternative heating and cooling), and a heating. The initial field test results indicate that the conventional BHE (W1) outperforms UTB during periods with low and continuous thermal load. However, when the building has short and high thermal loads for heating or cooling, UTB performs better than W1. A combination of a UTB and a conventional BHE (i.e., utilizing UTB to handle peak thermal loads and BHE to deal with base thermal loads) may provide better heat transfer performance than using either two BHEs or two UTBs.

## ACKNOWLEDGEMENT

This study is a part of research projects funded by the Building Technologies Office and Geothermal Technologies Office at the Department of Energy of the United States.

## REFERENCES

1. Liu, X., et al., Grid Cost and Total Emissions Reductions Through Mass Deployment of Geothermal Heat Pumps for Building Heating and Cooling Electrification in the United States. 2023: United States. p. Medium: ED; Size: 101 p.
2. Malhotra, M., et al., Heat pumps in the United States: Market potentials, challenges and opportunities, technology advances, in Conference: 14th IEA Heat Pump Conference - Chicago, Illinois, United States of America - 5/15/2023 4:00:00 AM-5/18/2023 4:00:00 AM. 2023: United States. p. Medium: ED.
3. Lu, Q., et al., Economic analysis of vertical ground source heat pump systems in Melbourne. Energy, 2017. **125**: p. 107-117.
4. Pokhrel, S., et al., Field-scale experimental and numerical analysis of a downhole coaxial heat exchanger for geothermal energy production. Renewable Energy, 2022. **182**: p. 521-535.
5. Saeidi, R., Y. Noorollahi, and V. Esfahanian, Numerical simulation of a novel spiral type ground heat exchanger for enhancing heat transfer performance of geothermal heat pump. Energy conversion and management, 2018. **168**: p. 296-307.
6. Yoon, S., S.-R. Lee, and G.-H. Go, Evaluation of thermal efficiency in different types of horizontal ground heat exchangers. Energy and Buildings, 2015. **105**: p. 100-105.
7. Acuña, J. and B. Palm. Comprehensive summary of borehole heat exchanger research at KTH. in IIR/Eurotherm sustainable refrigeration and heat pump technology conference. 2009.
8. Javadi, H., et al., Performance analysis of helical ground heat exchangers with different configurations. Applied Thermal Engineering, 2019. **154**: p. 24-36.
9. Wang, L., et al., Experimental Evaluation of Thermal Storage Performance of a Dual-Purpose Underground Thermal Battery. 2022, Oak Ridge National Lab.(ORNL), Oak Ridge, TN (United States).
10. Shi, L., et al., Numerical modeling and parametric study of a dual purpose underground thermal battery. Energy and Buildings, 2022. **275**: p. 112472.
11. Shi, L., et al., Development of New g-function Data for Simulating a Novel Shallow Bore Ground Heat Exchanger. 2022, Oak Ridge National Lab.(ORNL), Oak Ridge, TN (United States).
12. Wang, L., et al., Experimental Study on Charging and Discharging Performance of a Dual-Purpose Underground Thermal Battery. 2021, Oak Ridge National Lab.(ORNL), Oak Ridge, TN (United States).
13. Liu, X., et al., A Preliminary Study of a Novel Heat Pump Integrated Underground Thermal Energy Storage for Shaping Electric Demand of Buildings. 2019, Oak Ridge National Lab.(ORNL), Oak Ridge, TN (United States).